SAND2022-9804C

Evaluation of dynamically bi-orthonormal decomposition (DBO) for reduced order modeling (ROM) of compressible reacting flows with non-trivial boundary conditions

Swapnil Desai[1], Hessam Babaee[2], Jacqueline H. Chen[1]

[1]Sandia National Laboratories, USA, [2]University of Pittsburgh, USA

Background-Objective

Development of accurate predictive models in compressible reacting flows with a large number of species necessitates tracking every species by solving a separate transport equation. This can become computationally impracticable for complex fuels such as gasoline and diesel. At the same time, such flows are often characterized by the presence of strongly transient dynamical features associated with finite-time instabilities including auto-ignition, extinction, re-ignition etc. whose detection through infinite-time methods, e.g., long time averages or information about the statistical steady-state is not possible. In this work, the performance of dynamically bi-orthonormal (DBO) decomposition proposed by D. Ramezanian et al. (Comput. Methods Appl. Mech. Engrg. 382 (2021) 113882) is evaluated for the reduced-order modeling (ROM) of compressible reacting flows with non-trivial boundary conditions.

Numerical Method

The goal of DBO based ROM is to solve for a low-rank decomposition of species mass fraction matrix $Y(x,t)$ (where x denotes space and t denotes time) instead of solving the full-set of species transport equation:

$$\frac{\partial Y_i}{\partial t} = -\left(u\frac{\partial Y_i}{\partial x} + v\frac{\partial Y_i}{\partial y} + w\frac{\partial Y_i}{\partial z}\right) - \frac{1}{\rho}\left(\frac{\partial J_{i,x}}{\partial x} + \frac{\partial J_{i,y}}{\partial y} + \frac{\partial J_{i,z}}{\partial z}\right) + \frac{W_i\dot{\omega}_i}{\rho}$$

For details regarding the individual terms in the above equation, please refer to Chen et al., (Comp. Sci. Disc., 2 (2009) 015001). Note that the above equation and the conservative form of the species transport equation are equivalent. In a DBO based ROM simulation, after evolving the above equation in time for a certain number of time steps, the singular value decomposition (SVD) of the $Y(x,t)$ matrix is performed to obtain U, Σ and V^T as shown in Figure 1.

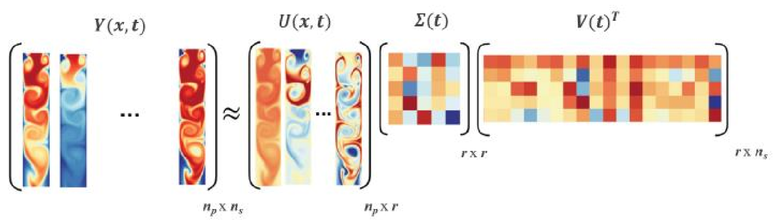

Figure 1. Schematic of dynamically bi-orthonormal decomposition of species matrix $Y(x,t)$. Adopted from D. Ramezanian et al. (Comput. Methods Appl. Mech. Engrg. 382 (2021) 113882)

$U(x,t)$ in Fig. 1 represents a set of orthonormal spatial modes, $\Sigma(t)$ is a factorization of the low-rank correlation matrix and $V(t)$ is the orthonormal species modes matrix representing a low-dimensional time-dependent manifold of the full composition space. In the decomposition shown in Fig. 1, n_s represents the number of species, r is the rank of DBO and n_p is the total number of grid points. The closed form evolution of equations for the components of the DBO decomposition are based on the variational principle that seek to optimally update the DBO components given the change in the right hand side of the species transport equation while preserving orthonormality constraints. For compressible reacting flows, these equations are presented as follows:

$$\frac{\partial U}{\partial t} = \prod_{\perp U}\left[-\left(u\frac{\partial U}{\partial x} + v\frac{\partial U}{\partial y} + w\frac{\partial U}{\partial z}\right) - \frac{1}{\rho}\left(\frac{\partial J_{i,x}V}{\partial x} + \frac{\partial J_{i,y}V}{\partial y} + \frac{\partial J_{i,z}V}{\partial z}\right)\Sigma^{-1} + \frac{W_i\dot{\omega}_i}{\rho}V\Sigma^{-1}\right] \rightarrow PDE$$

$$\frac{d\Sigma}{dt} = -\left\langle U, u\frac{\partial U}{\partial x} + v\frac{\partial U}{\partial y} + w\frac{\partial U}{\partial z}\right\rangle\Sigma + \left\langle U, \frac{\partial J_{i,x}V}{\partial x} + \frac{\partial J_{i,y}V}{\partial y} + \frac{\partial J_{i,z}V}{\partial z}\right\rangle + \left\langle U, \frac{W_i\dot{\omega}_i}{\rho}V\right\rangle \rightarrow ODE$$

$$\frac{dV}{dt} = \prod_{\perp V}\left[\left\langle \frac{\partial J_{i,x}}{\partial x} + \frac{\partial J_{i,y}}{\partial y} + \frac{\partial J_{i,z}}{\partial z}, U\right\rangle + \left\langle \frac{W_i\dot{\omega}_i}{\rho}, U\right\rangle\right]\Sigma^{-T} \rightarrow ODE$$

Here, $\langle\,\rangle$ denotes inner product either between two scalar fields or two matrices. The operators $\prod_{\perp U}$ and $\prod_{\perp V}$ are defined as:

$$\prod_{\perp U} f = f - U\langle U, f\rangle \text{ and } \prod_{\perp V} f = f - VV^T f$$

The main advantage of using DBO is that the transport partial differential equation (PDE) is solved only for r spatial modes as opposed to n_s species in the full-set of transport equations. The computational cost of evolving Σ and V is negligible as they are governed by low-rank ordinary differential equations (ODEs). Moreover, since the species are stored in *compressed* form in DBO, i.e. U, Σ and V are kept in memory instead of their multiplication $U\Sigma V^T$ i.e. the *decompressed* form, a memory compression ratio of n_s/r is achieved. At $t = 0, r = 1$ for the majority of initial conditions. If $r > 1$ is chosen in DBO at $t = 0$, the matrix $\Sigma(t)$ becomes singular. Therefore, the full-set of species transport equation is evolved first for a specified physical time to allow the reacting flow to develop so that the rank r increases and the matrix $\Sigma(t)$ becomes non-singular.

Boundary Treatment

The DBO formulation allows a non-intrusive way of implementing the Navier-Stokes Characteristics Boundary Conditions (NSCBCs) that are typically used in compressible reacting flow solvers. In a DBO based ROM simulation, it can be applied by adopting the following steps:

1) Construct the right hand side of the full-set of species transport equations shown below:

$$\mathrm{RHS}_{Boundary} = \left[-\left(u\frac{\partial Y_i}{\partial x} + v\frac{\partial Y_i}{\partial y} + w\frac{\partial Y_i}{\partial z}\right) - \frac{1}{\rho}\left(\frac{\partial J_{i,x}}{\partial x} + \frac{\partial J_{i,y}}{\partial y} + \frac{\partial J_{i,z}}{\partial z}\right) + \frac{W_i\dot{\omega}_i}{\rho}\right]$$

2) Use the specific LODI relation to express the incoming waves (L_{5+i}) as a function of the corresponding outgoing waves

$$\text{LODI Relation: } \frac{\partial Y_i}{\partial t} + L_{5+i} = 0 \text{ where } L_{5+i} = u\frac{\partial Y_i}{\partial x}$$

3) Correct $\mathrm{RHS}_{boundary}$ based on the values of L_{5+i} and evolve the spatial mode U at the boundary as follows:

$$\frac{\partial U_{Boundary}}{\partial t} = \prod_{\perp U}\left[\mathrm{RHS}_{Boundary}V\Sigma^{-1}\right]$$

4) Since Σ and V are independent of space, no changes are required in their respective evolution equations.

Demonstration Case 1

(End-gas Auto-ignition to Detonation Transition)

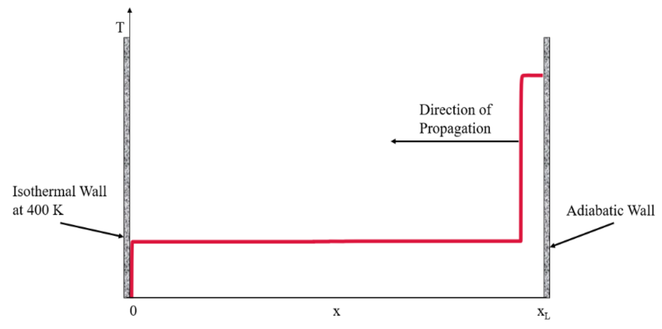

Figure 2. Initial temperature profile of the 1-D end-gas auto-ignition to detonation transition case

Case Details

- Stoichiometric gasoline surrogate/air mixture at T_u = 1100 K and P = 35 bar
- 39 species Shell-D/air mechanism by Xu et al (Combust. Flame, 220 (2020) 475-487)
- x_L = 1 cm, 6 μm grid resolution, iso-thermal wall at 400 K on the left boundary and adiabatic wall on the right boundary
- Simulations performed with the DNS code S3D
  - 8th order finite difference operator for diffusive fluxes
  - 7th order WENO operator for convective fluxes
  - 4th order, 6-stage explicit Runge-Kutta time integrator
  - LAPACK library for linear algebra operations
- DBO simulation started at t = 0

Temporal evolution of thermodynamic scalars

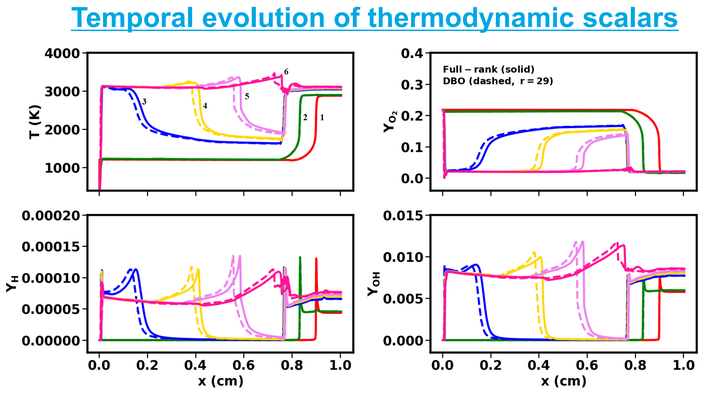

Figure 3. Temporal evolution of temperature and mass fractions (Y) of O_2, H and OH obtained with full-rank simulation (solid lines) and low-rank (r = 29) DBO simulation (dotted lines). Numbers labeling each temperature profile indicate the time sequence.

- Accurate prediction of flame propagation speed and onset of end-gas auto-ignition with DBO - ROM
- Accurate prediction of temporal evolution of species mass fractions (Y) orders of magnitude apart from one another
- Differences in the propagation speed of the short lived auto-ignition front and peak pressure (Full-rank ~ 242 bar, DBO-ROM ~ 235 bar)
- State variables at the boundaries physically consistent with the chosen boundary conditions
- Overall, DBO-ROM reasonably estimates the full-rank temperature and species mass fraction trends with r = 29 which corresponds to approximately 74% of the total species count in the employed mechanism
- Required wall-clock time approximately the same between DNS and DBO-ROM but 26% reduction in memory footprint

Temporal evolution of error in DBO-ROM

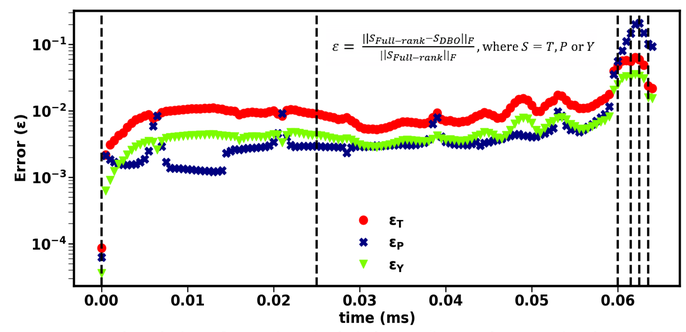

Figure 4. Temporal evolution of error in T (red circles), Y (inverted green triangles) and P (blue crosses) in DBO-ROM compared to full-rank simulation. Dotted vertical lines correspond to the instantaneous error in respective variables at specific times (profiles 1 – 6) depicted in Figure 3.

- Relative error gradually increases over time but remains between 10^{-2} and 10^{-3} for majority of the simulation period

Demonstration Case 2

(Premixed Flame/Wall Interaction)

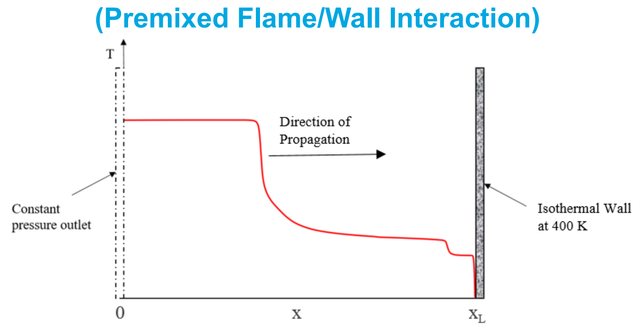

Figure 5. Initial temperature profile of the 1-D premixed flame/wall interaction case

Case Details

- Lean n-heptane/air two-staged flame at Tu = 800 K, P = 40 bar and ø = 0.6, 52 species n-heptane/air mechanism by Lu et al. (Combust Flame, 156 (2009), 1542-1551)
- x_L = 2 cm, 10 μm grid resolution, constant pressure outlet on the left boundary and iso-thermal wall at 400 K on the right boundary, DBO simulation started at t = 0.5 ms

Temporal evolution of thermodynamic scalars

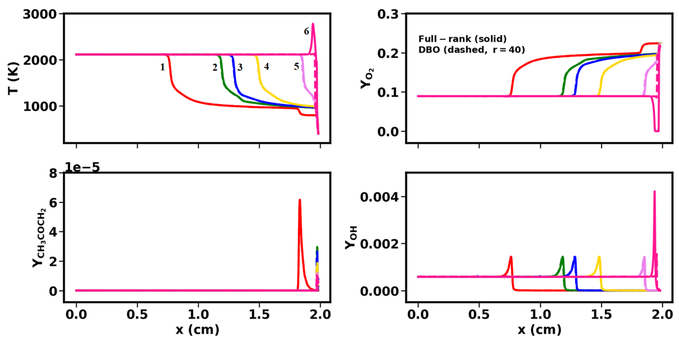

Figure 6. Temporal evolution of temperature and mass fractions of O_2, CH_3COCH_2 (low-T chemistry) and OH (high-T chemistry) obtained with full-rank simulation (solid lines) and low-rank (r = 40) DBO simulation (dotted lines). Numbers labeling each temperature profile indicate the time sequence.

- Accurate prediction of flame propagation speed, cool flame quenching as well as temporal evolution of species mass fractions (Y) orders of magnitude apart from one another
- Differences in the hot-flame quenching event at wall. Overall, DBO-ROM able to reasonably estimate the full-rank temperature and species mass fraction trends with r= 40 or approximately 76% of the total species count

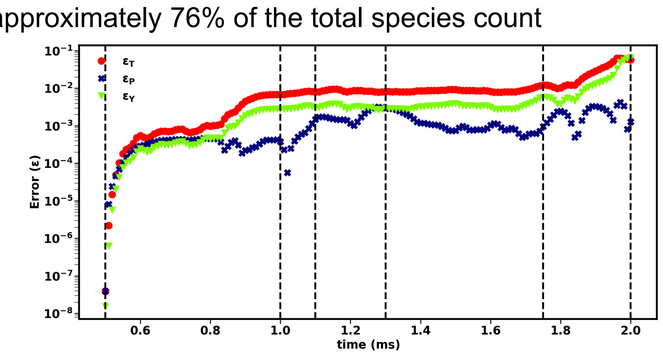

Figure 7. Temporal evolution of error in T (red circles), Y (inverted green triangles) and P (blue crosses) in DBO-ROM compared to full-rank simulation. Dotted vertical lines correspond to the instantaneous error in respective variables at specific times (profiles 1 – 6) depicted in Figure 6.

- As observed in Case-1, the relative error gradually increases over time but remains between 10^{-2} and 10^{-3} for the majority of the simulation period

Remark on accuracy

Error accumulates over time in each case due to lost interactions of DBO modes with unresolved modes. The DBO can be augmented with an adaptive strategy to add/remove modes based on a criterion for overcoming this issue.

Conclusion

The effectiveness of DBO based ROM in efficiently tackling high dimensionality related to simulating compressible reacting flows with non-trivial boundary conditions is demonstrated here. As such, future implementation of DBO for simulation of complex turbulent combustion systems is warranted.

Sandia National Laboratories

University of Pittsburgh

Acknowledgements: The work at Sandia was supported by the US Department of Energy, the Exascale Computing Project (17-SC-20-SC), and the Office of Science Distinguished Scientists Fellows Award.. Sandia National Laboratories is a multi-mission laboratory managed and operated by National Technology and Engineering Solutions of Sandia, LLC., a wholly owned subsidiary of Honeywell International, Inc., for the U.S. Department of Energy's National Nuclear Security Administration under contract DE-NA- 0003525